Diagnosis of Injury to Axially Impacted Foot-Ankle-Leg Complexes by Use of Dermestidae

B. J. Perry[1], S. H. Sochor[1], and R. S. Salzar[1]
[1] University of Virginia, Center for Applied Biomechanics

ABSTRACT

Conflicts in the Gulf have exposed warfighters to injury by means of improvised explosive device (IED) detonation beneath armored military vehicles, commonly referred to as underbody blast (UBB). Together with the pelvis, injuries to the foot-ankle-leg number among those most commonly sustained by warfighters in the event of a UBB. Multiple biomechanical tests are currently being conducted in order to develop injury thresholds and risk functions for warfighters subjected to these vertical loads. In a previous study of 38 foot-ankle-leg complexes tested under automotive and UBB load rates, a distribution of injuries was produced. High-speed x-ray video and post-test CT, Statscan (Lodox, Johannesburg, South Africa), and dissection were performed to document injuries. It is, however, difficult to thoroughly remove soft tissue and cartilage from the calcaneus and talus without inducing damage that could be mistaken as a test-induced injury. For this test series, Dermestidae macerated 32 tali and 18 calcanei revealing 12 and 4 injuries, respectively, that were previously undiagnosed through more traditional techniques. Logistic regressions were produced to quantify the significance of the findings. The pre- and post-maceration regressions predicted a 50% injury risk of 6626N and 4228N, respectively, or a 44% difference in mean.

INTRODUCTION

Gulf conflicts have given rise to warfighter injury by means of improvised explosive device (IED) detonation beneath armored military vehicles, commonly referred to as underbody blast (UBB). Ramasamy reported that 81% of warfighter-sustained injuries caused by UBB experienced injury to the foot-ankle-leg (Ramasamy, 2011). These injuries, though in many cases not directly life threatening, are severely debilitating and costly in terms of quality of life, can cause immediate functional capacity degradation such as post-blast evacuation.

In a previous study, post mortem human subject (PMHS) foot-ankle-leg complexes were tested axially to simulate loading conditions produced by automotive intrusion (AI) and UBB (Figure 1) (Bailey, 2017). To summarize that study, 38 specimens were fixed at the knee and tested at three input conditions with accelerations of 7.3g in 7.60ms, 75.1g in 3.48ms, and 192.3g in 3.50ms. Twelve specimens were tested at each condition with two additional specimens tested at the low condition wearing the Thor Dummy shoe (Ridella, 2011). The goal of that study was to

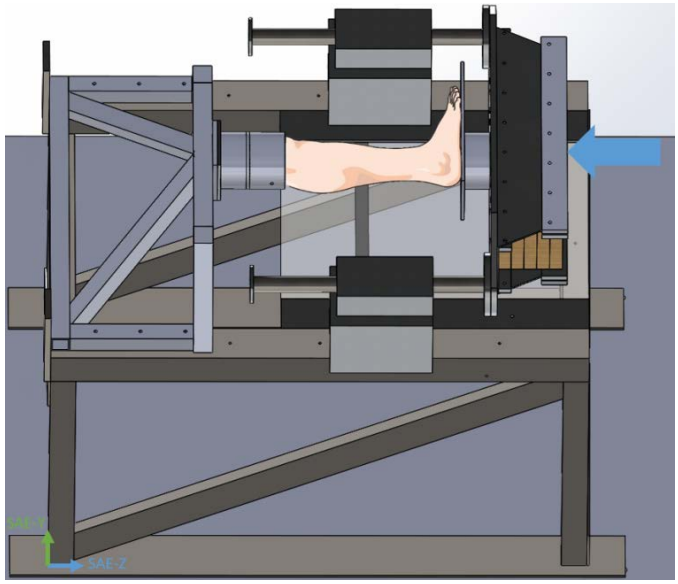

Figure 1: Schematic of the test rig used to axially impact the foot-ankle-leg complexes. The blue arrow indicates loading direction.

evaluate loading duration and rate on the fracture force of foot-ankle-leg complexes. The inputs typically produced injuries to the calcaneus, talus, tibia, fibula, navicular, and cuboid with a range of severity. Thorough documentation of injuries is paramount to produce accurate statistical models such as survival and injury risk functions and injury thresholds. Techniques including high-speed x-ray video, post-test CT (GE Healthcare Optima CT660, Boston, Massachusetts), Statscan (Lodox, Johannesburg, South Africa), and dissection were used to document injuries.

The calcaneus contains attachments to numerous ligaments and tendons, making it a daunting task to sufficiently denude the bone in order to inspect for injury. Since the calcaneus is primarily composed of trabecular bone surrounded by a thin, fragile cortical shell, the act of removing the periosteum can readily induce damage (Hall, 1993). The talar surface is almost entirely enveloped with a thick layer of articular cartilage, potentially concealing hairline and other less severe fractures. In removing this tissue, it is common to cut into the bone while dissecting, making it difficult to distinguish between injury and artifact.

X-ray, computed tomography (CT), magnetic resonance imaging (MRI), and ultrasound have been used to detect injury in nearly every body region (Jacob, 2013). Clinically, there are radiation limits that cannot be exceeded, hindering the ability of CT and x-ray to detect less severe fractures. For this study, radiation dosage was not a concern so maximum exposure, 0.625mm slice and interval thickness, was used for CT. MRI is inherently better suited to image soft tissue than bone and is rarely used as a skeletal injury detection technique in the Biomechanics and Medical fields. Bozorgi evaluated the ability of ultrasound as compared to radiography to detect fracture in various body regions with mixed results (Bozorgi, 2017). This study showed a success rate of 100% for femur fracture but only 48% for intra-articular fractures.

A maceration technique that sufficiently denudes bones to allow for injury identification, and preserves mechanical properties of bone for later testing, was necessary. Steadman discussed

six maceration categories, most of which include chemicals or heat that potentially precludes the mechanical testing of the bone for material properties (Steadman, 2006). Invertebrate maceration was noted as a category that has little effect on bone. For this study, a family of flesh eating beetles known as Dermestidae were employed to evaluate their ability to rid bones of soft tissue and cartilage, and to expose any hidden fractures. Four parametric regression distributions were used to evaluate the pre- and post-maceration datasets.

METHODS

All specimens included in this study were previously tested (Bailey, 2017). Post-test CT scans were performed on the specimens tested at the intermediate and high input condition. Statscan images only were taken for the subjects tested at the low input condition as those specimens were well below the known injury threshold. Scans were reviewed by Center researchers, but not given to a radiologist. All specimens were carefully dissected post scan. Subcutaneous cuts to the dermis were made with a scalpel while surgical scissors were used to cut ligaments and tendons to extract the calcaneus, talus, navicular, and cuboid. Surgical scissors and bone tomes were used to remove soft tissue from the tibia and fibula. Bones pending maceration were wrapped in gauze, soaked in saline, and stored at 1°C. Specimens were macerated individually to ensure bones were properly denuded.

Approximately 1500 Dermestidae were acquired to begin the colony (Figure 2). The colony was housed in a 10-gallon glass reptile aquarium in an area that receives little light. The aquarium was layered with two inches of natural small pet paper bedding. Moisture levels were maintained by daily spritzing of the bedding material. Care was taken to avoid saturation as mold can become an issue and eliminate the colony (Anderson, 2013).

Figure 2: Dermestidae upon receipt.

All PMHS testing at the University of Virginia is classified as Biohazard Safety Level II by the UVA Institutional Biosafety Committee, and thus containment of the Dermestidae was crucial in order to manage the biological material risk. Dermestidae are known to freely climb the silicon seals at the corners of an aquarium, so metallic tape was placed over the bead. Dermestidae can also develop wings and fly if food becomes scarce and the temperature exceeds 27°C (Kodiak Bones and Bugs Taxidermy).

A thermostatically controlled heating element adhered to the underside of the aquarium maintained the temperate at no higher than 24°C. The colony was fed with a constant source of bologna until approximately 20 grams of bologna was consumed in a 24-hour period. At that point, it was estimated that the colony would be able to macerate specimens in a similar time period. The colony was again fed bologna when specimens weren't available.

Achilles' tendons were not readily consumed so they were trimmed, prior to introduction into the aquarium, with kitchen shears. Initially, the distal tibia and inferior calcaneus were sectioned to be denuded by the Dermestidae, but resulted in their burrowing into the exposed trabeculae and perishing. For this study, the majority of bones macerated were calcanei and tali. Navicular, cuboid, and cuneiform injuries were not common, therefore, these bones were typically not macerated. One navicular was macerated due to observed articular cartilage displacement without visible cortical damage.

All bones were macerated for 24 hours, afterwards wrapped in gauze, and stored in saline at 1°C, which was sufficient to terminate any embryos or larvae that remained on the specimens. Prior to inspection, bones were treated with a thin application of India ink to aid in exposing any fine cracks or abrasions. Injury was defined as any disruption to cortical bone. Upon completion of the study, the Dermestidae, along with the aquarium, were placed in a freezer for 72 hours with the remains disposed of in regulated medical waste.

Weibull (Equation 1), logistic (Equation 2), normal (Equation 3), and lognormal (Equation 4) distributions were calculated for the pre- and post-maceration datasets using Minitab statistical software version 17 (Minitab, Inc., State College, PA). The Weibull cumulative density function (CDF) takes the form

$$F(x) = 1 - e\left[-\left(\frac{x}{\alpha}\right)^{\beta}\right] \qquad (1)$$

where α is the scale parameter and β is the shape parameter; the logistic CDF is

$$F(x) = \frac{1}{1 + e\left[\frac{-(x-\mu)}{\sigma}\right]} \qquad (2)$$

where μ is the location and σ is the scale parameter; the normal CDF has an integral form

$$F(x) = \int_{-\infty}^{x} \frac{1}{\sigma\sqrt{2\pi}} e\left[-\frac{(t-\mu)^2}{2\sigma^2}\right] dt \qquad (3)$$

where μ is the location and σ is the scale parameter; the lognormal CDF also has in integral form

$$F(x) = \int_{-\infty}^{x} \frac{1}{t\sigma\sqrt{2\pi}} e\left[-\frac{(\ln(t)-\mu)^2}{2\sigma^2}\right] dt \qquad (4)$$

where μ is the location and σ is the scale parameter. All equations were provided by Minitab.

The statistical models were calculated assuming arbitrary censoring. Regressions were compared using the Anderson-Darling (A-D) statistic (Stephens, 1974). The A-D statistic quantifies the "goodness of fit" of a specific regression to a given dataset, weighting the squared distance between individual data points and the statistical model, while providing more emphasis at the tails. The regression distribution that produced the smallest summed A-D scores from pre- and post-maceration was used to compare statistical differences between the two injury datasets.

Specimens excluded from regression analysis are 545R and 647L as these legs were impacted twice. Specimens 577L and 647R were also excluded because those specimens were tested wearing the Thor dummy shoe, providing a different boundary condition. Overall, 34 specimens were used for regression analysis.

RESULTS

Documented injuries and tissue macerated by Dermestidae are outlined in Table 1. There were 26 calcaneus, 14 tibia, 22 talus, 9 fibula, 5 navicular, and 1 cuboid injury for a total of 77. Of those injuries, Dermestidae aided in diagnosing 4 calcaneus, 12 talus, and 1 navicular injury that were previous undiagnosed. Out of the 34 specimens used for regression analysis, six changed from no injury to injury, post-maceration (Table 2).

An example of these injuries and Statscan can be found in Figure 3. Of the four regression distributions compared (Table 3), the logistic distribution proved to be the most accurate (Figure 1). Input data and results for the pre- and post-maceration regression analysis are provided in Table 2 and Table 4, respectively.

DISCUSSION

Traditional injury detection methods such as post-test CT or Statscan and dissections were performed on each tested specimen. To the author's knowledge, this was the first study to use high-speed x-ray video for fracture detection. In general, high speed x-ray had greater value in

Table 1: Injuries produced by Bailey, et al [2]. Cells that contain a "y" and are not highlighted indicate injuries diagnosed by traditional dissection methods or x-ray. Highlighted cells with a "y" indicate previously undiagnosed injuries revealed by Dermestidae maceration.

Input Condition	Specimen #	Calcaneus	Tibia	Talus	Fibula	Navicular	Cuboid	Macerated Tissue
Low	529L	y	n	y	n	n	n	Calcaneus and Talus
	529R	n	n	y	n	n	n	Calcaneus and Talus
	532R	y	n	y	n	n	n	Calcaneus and Talus
	545R*	y	n	n	y	y	n	Talus
	546L	n	n	y	n	n	n	Calcaneus and Talus
	577R	n	n	n	n	n	n	Calcaneus and Talus
	579L	n	n	n	n	n	n	Calcaneus and Talus
	647L*	n	y	y	y	n	n	Calcaneus and Talus
	674L	y	n	y	n	n	n	Calcaneus and Talus
	674R	y	n	n	n	n	n	Calcaneus and Talus
	695L	n	n	n	n	n	n	Calcaneus and Talus
	695R	n	n	n	n	n	n	Calcaneus and Talus
Low w/ shoe	577L	n	n	n	n	n	n	Calcaneus and Talus
	647R	n	n	n	n	n	n	Calcaneus and Talus
Intermediate	538R	y	y	y	n	n	n	Inferior Calcaneus and Distal Tibia
	539L	y	y	n	n	n	n	Inferior Calcaneus and Distal Tibia
	541R	n	y	y	n	n	n	Calcaneus and Talus
	542R	n	y	n	y	n	n	Calcaneus and Talus
	554R	y	n	y	n	n	n	Talus
	555L	y	n	n	n	n	n	Talus
	565R	y	y	n	n	n	n	Talus
	573L	y	n	y	y	n	n	Talus
	574R	y	y	y	n	n	n	Talus
	575L	y	n	y	n	n	n	NA
	576R	n	n	n	n	n	n	Calcaneus and Talus
	578L	y	y	y	n	n	n	Calcaneus
High	538L	y	y	y	y	y	y	NA
	539R	y	y	n	n	n	n	Calcaneus and Talus
	541L	y	y	y	y	n	n	Talus
	542L	y	n	n	y	y	n	Talus
	554L	y	n	y	n	y	n	Talus and Navicular
	555R	y	n	y	n	n	n	Talus
	565L	y	y	y	n	n	n	Talus
	573R	y	n	y	y	y	n	NA
	574L	y	y	y	n	n	n	Talus
	575R	y	y	y	y	n	n	NA
	576L	y	n	n	n	n	n	Talus
	578R	y	n	y	n	n	n	Talus

*Indicates specimens that were retested to determine the high input condition.

fracture timing than fracture detection as injuries detectable by this method were easily discernable by CT or dissection.

Although the subjects tested at the low condition were scanned with plane x-ray, the injuries diagnosed post-maceration were similar to those observed at the higher input conditions, which were CT scanned. Due to similarities, it is assumed that the low condition post-maceration diagnosed injuries would have also gone undiagnosed if post-test CT scanned. It can be concluded that injuries diagnosed post-maceration were not caused by Dermestidae as comparable injuries were often diagnosed during dissection.

Table 2: Input data for regression analysis, pre- and post-maceration.

Specimen Number	Peak Force [N]	Pre-Maceration	Post-Maceration
529L	-3019.63	0	1
529R	-3253.18	0	1
532R	-3217.67	0	1
546L	-3464.16	0	1
577R	-3561.03	0	0
579L	-4755.06	0	0
674L	-3662.31	0	1
674R	-4460.95	0	1
695L	-4394.8	0	0
695R	-2885.9	0	0
538R	-9629.3	1	1
539L	-9207.12	1	1
541R	-9499.92	1	1
542R	-12835.4	1	1
554R	-8463.86	1	1
555L	-6882.89	1	1
565R	-12110.8	1	1
573L	-8386.74	1	1
574R	-7453.84	1	1
575L	-10696.2	1	1
576R	-13269.9	0	0
578L	-10743.1	1	1
538L	-11772.4	1	1
539R	-14298.8	1	1
541L	-10153	1	1
542L	-12844	1	1
554L	-9129.23	1	1
555R	-9765.22	1	1
565L	-11384.5	1	1
573R	-10017.2	1	1
574L	-9249.19	1	1
575R	-13190	1	1
576L	-17822.8	1	1
578R	-10579.9	1	1

Typically, injuries diagnosed post-maceration were disruptions to the cortical shell, beneath articular cartilage. According to the Abbreviated Injury Scale (AIS) and the Ankle and Foot Injury Scale-Severity (AFIS-S), all injuries diagnosed due to Dermestidae maceration were a 2 and a 3, respectively, indicating moderate injuries (Committee on Injury Scaling, 2005), (Levine, 1995).

Overlap in the 95% confidence intervals for the pre- and post-maceration logistic regressions is apparent, however, the locations, or means, have a 44% difference (Table 4). The pre-maceration regression has a fiftieth percentile risk of 6626N, which equates to approximately 80% probability of fracture, according to the post-maceration regression.

Figure 3: Representative talus (top) and calcaneus (middle) injuries diagnosed after maceration along with post-test Statscan (bottom). This particular specimen is 674L.

A two-tailed McNemar's test was used to evaluate the difference between pre- and post-maceration datasets, proving statistical significance ($p<0.05$). A two-tailed test was opted for as there may be scenarios in which an injury is suspected with CT but not diagnosed post-maceration. For this study, all injuries diagnosed by CT were discernable during dissection, pre-maceration.

CONCLUSIONS

Post-test CT, Statscan, and dissections were insufficient in detecting all injuries as nearly one quarter of all injuries were diagnosed post-maceration. The authors acknowledge that scans

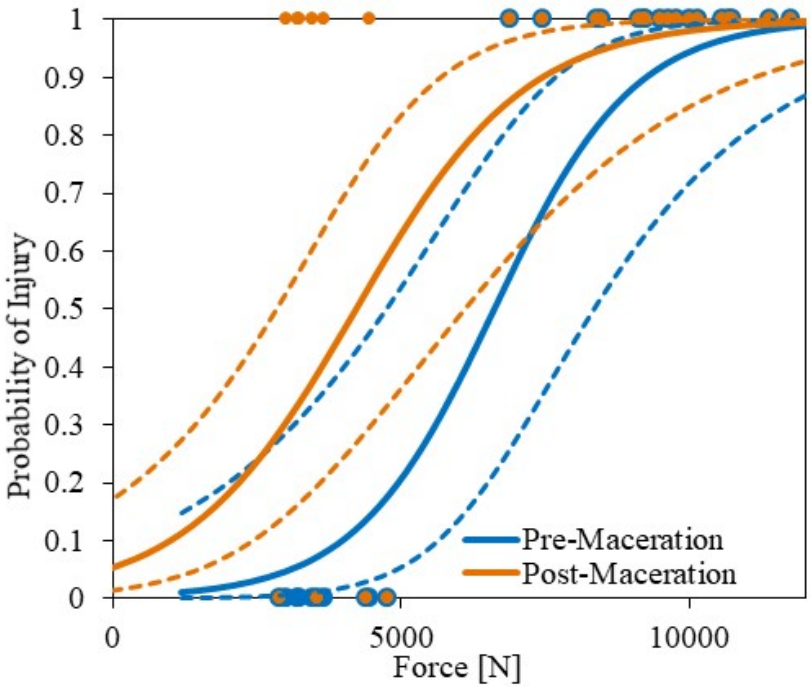

Figure 4: Logistic regressions for pre- and post-maceration injury datasets. Dashed lines indicate 95% confidence intervals.

were not reviewed by a trained radiologist. To be thorough, all injuries diagnosed after maceration were reviewed in CT or Statscan without successful diagnosis.

Most injuries diagnosed post-maceration were mere millimeters in length. Although the specimens tested at the intermediate and high input condition were CT scanned with 0.625mm slice and interval thickness and dissected, seven injuries were diagnosed due to Dermestidae (Table 1). The six specimens that changed from no injury to injury after maceration were all tested at the low input conditions.

PMHS injury detection is an arduous task and subtle injuries are often overlooked, especially those beneath articular cartilage. This study provides evidence of the difficulty in documenting all injuries in the foot and ankle and the consequences of overlooking injuries.

Table 3: Regression distribution Anderson-Darling scores for pre- and post-maceration datasets.

Dataset	A-D Score			
	Weibull	Normal	Lognormal	Logistic
Pre-	0.409	0.822	1.555	0.772
Post-	1.688	0.381	0.452	0.401
Sum	2.097	1.203	2.007	1.173

Table 4: Logistic regression results for pre- and post- maceration datasets.

Dataset	Location [N]	Scale [N]	Standard Deviation [N]
Pre-	6626	1198	2174
Post-	4228	1465	2658

ACKNOWLEDGEMENTS

This study was self-funded by the University of Virginia Center for Applied Biomechanics. The authors thank the Center for Applied Biomechanics Biological Protocol Committee for their help and support.

REFERENCES

ANDERSON, B. (2013). Dermestid Beetle Care Sheet. https://dermestidbeetles.files.wordpress.com/2013/01/dermestid-beetle-care-sheet.pdf.

BAILEY, A.M., PERRY, B.J., SALZAR, R.S. (2017). Response and injury of the human leg for axial impact durations applicable to automotive intrusion and underbody blast environments. International Journal of Crashworthiness, 1–9.

BOZORGI, F., AZAR, M.S., MONTAZER, S.H., CHABRA, A., HEIDARI, S.F., KHALILIAN, A. (2017). Ability of Ultrasonography in Detection of Different Extremity Bone Fractures; a Case

Series Study. Emergency, 5(1). https://www.ncbi.nlm.nih.gov/pmc/articles/PMC5325883/, April 7, 2017.

COMMITTEE ON INJURY SCALING. (2005). *Abbreviated Injury Scale*. Association for the Advancement of Automotive Medicine.

HALL, R.L., SHEREFF, M.J. (1993). Anatomy of the Calcaneus. Clinical orthopaedics and related research, 290, 27–35.

JACOB, N.E., WYAWAHARE, M.V. (2013). Survey of Bone Fracture Detection Techniques. International Journal of Computer Applications, 71(17), 31–34.

Kodiak Bones and Bugs Taxidermy. http://www.bonesandbugs.com/dermestid-beetles-faqs.html, May 1, 2017.

LEVINE, R., MANOLI II, A., PRASAD, P. (1995). Ankle and Foot Injury Scales. American Orthopaedic Foot and Ankle Society, 355–362.

RAMASAMY, A., MASOUROS, S.D., NEWELL, N., HILL, A.M., PROUD, W.G., BROWN, K.A., et al. (2011). In-vehicle extremity injuries from improvised explosive devices: current and future foci. Philosophical Transactions of the Royal Society B: Biological Sciences, 366(1562), 160–170.

RIDELLA, S., PARENT, D. (2011). Modifications to improve the durability, usability, and biofidelity of the THOR-NT dummy. 22nd ESV Conference, Paper. https://www-nrd.nhtsa.dot.gov/Pdf/ESV/esv22/22ESV-000312.pdf, May 1, 2017.

STEADMAN, D.W., DIANTONIO, L.L., WILSON, J.J., SHERIDAN, K.E., TAMMARIELLO, S.P. (2006). The Effects of Chemical and Heat Maceration Techniques on the Recovery of Nuclear and Mitochondrial DNA from Bone*. Journal of Forensic Sciences, 51(1), 11–17.

STEPHENS, M.A. (1974). EDF Statistics for Goodness of Fit and Some Comparisons. Journal of the American Statistical Association, 69(347), 730–737.